Technical University of Denmark

DTU

AFG-MONSU. A program for calculating axial heterogeneities in cylindrical pin cells

Neltrup, H.; Kirkegaard, Peter

Publication date:
1978

Document Version
Publisher's PDF, also known as Version of record

Link back to DTU Orbit

DTU Library
Technical Information Center of Denmark

Risø

Title and author(s)	Date August 1978
AFG-MONSU. A Program for Calculating Axial Heterogeneities in Cylindrical Pin Cells by H. Neltrup and P. Kirkegaard	**Department or group** Department of Reactor Technology
	Group's own registration number(s)
pages + tables + illustrations	

Abstract

	Copies to

The AFG-MONSU program complex is designed to calculate the flux in cylindrical fuel pin cells into which axial heterogeneities are introduced in a regular array.

The theory - integral transport theory combined with Monte Carlo by help of a super-position principle - is described in some detail.

Detailed derivation of the superposition principle as well as the formulas used in the DIT (Discrete Integral Transport) method is given in the appendices along with a description of the input structure of the AFG-MONSU program complex.

1. INTRODUCTION

The AFG-MONSU program complex is designed to calculate the flux in cylindrical fuel pin cells into which axial heterogeneities are introduced. The heterogeneity consists in changing the composition of a central cylindrical region in axial intervals repeated regularly along the axis.

The purpose of this procedure is to calculate the effect of introducing a regular array of poisoned fuel pellets separated by normal fuel pellets.

The solution is obtained by application of a superposition principle proposed by B. Fredin (1) which transfers the problem into one excellently suited for Monte Carlo calculation.

2. THE SUPERPOSITION PRINCIPLE

2.1. The general principle

The principle can be formulated on a quite general form.

Suppose a stationary solution to the neutron transport equation exists in an arbitrary material configuration subject to a suitable boundary condition.

A certain material composition, A, exists in subvolume V inside surface S. The flux, as a function of position vector $\underline{r}$ and direction $\underline{\Omega}$ in all space , is called ϕ^A. Now the material composition inside S is changed to another composition, B, for which a stable solution ϕ^B exists in all space .

Then if A and B do not imply any sources inside V the solution ϕ^B may be expressed as

1. For r ∈ V

$$\phi^B = \phi_B(Q_s) \tag{2.1.1}$$

where ϕ_B is the solution in all space with material configuration B inside V derived from a surface source on S

$$Q_s = \phi^A(\underline{r}, \underline{\Omega}) \, (\underline{n} \cdot \underline{\Omega}) \qquad r \in S \tag{2.1.2}$$

$\underline{n}$ is the vector normal to S and directed into V. All other sources are ignored in the calculation of $\phi_B(Q_s)$.

2. For $r \notin V$

$$\phi^B = \phi_B(Q_s) + \phi^A \tag{2.1.3}$$

A formal proof, which has been worked out by G.K. Kristiansen, is given in Appendix I.

2.2. The practical application

In the practical application the ordinary flux solution in the cylindrical symmetric fuel pin cell is first obtained by integral transport theory. From the solution the angular flux on the surface of the poisoned pellets as expressed by the first six components of its spherical harmonic expansion is derived by integration from the centre of the cell. This part of the calculation is performed by the program AFG (Angular Flux Generator). The flux found by AFG is the multigroup solution of the pin cell eigenvalue problem.

The angular components are used as weights for starters, Q_s, on the surface of the poison pellets in the subsequent Monte Carlo calculation of $\phi_B(Q_s)$, which is performed by the program MONSU (Monte Carlo Superposition). The multigroup Monte Carlo treatment takes place only in the thermal groups. This means that no sources appear inside the poison volume V except slowing down from epithermal, which may be neglected. The slowing down sources in the moderator appears only indirectly through the thermal flux solution ϕ^A from AFG. This implies the following assumptions. 1) No slowing down source in the fuel-(poison-)region, 2) The distribution of thermal slowing down sources in the moderator is not influenced by the change in the fission distribution caused by the introduction of the poison. 3) No absorption by the poison in the non-thermal groups.

When $\phi_B(Q_s)$ has been calculated the flux in the poisoned cell ϕ^B is calculated through (2.1.1) and (2.1.3). The eigenvalue k_{eff} in the AFG solution is found as the ratio between the total number of fissions and absorptions. When ϕ^B has been found, new values of absorption and fission in the thermal groups can

be determined, by which the change in k_{eff} under assumptions 1,
2 and 3 can be estimated.

3. THE AFG PROGRAM

3.1. General formulation

The program solves the neutron transport problem in cylinder
geometry by use of integral transport theory applying the so-
called DIT (Discrete Integral Transport) method originally pro-
posed by Kobayashi and Nishihara (2) and further developed by
Carlvik (3).

The problem solved in each energy group can be formulated
in the following way

$$\phi(r) = \int_0^R 2\pi r' \, Q(r') \, T(r,r') \, dr' \tag{3.1.1}$$

$\phi(r)$ is the flux at radius r, $Q(r') = \phi(r') \, \Sigma_s + S(r')$ on the
right side is the emission density. The source term, $S(r')$ may
have contributions from both up- and down-scattering from other
groups as well as fission.

3.2. The black boundary condition

The calculation of the transfer kernel $T(r,r')$ goes by way of
first considering the case where the cell boundary (r = R) is
black.

As shown in Appendix II the corresponding transfer kernel
$T_b(r,r')$ may be written

$$T_b(r,r') = 1/(4\pi^2) \int_{-r_{least}}^{r_{least}} (Ki1(\tau(\rho_1))$$

$$+ Ki1(\tau(\rho_2)))/(SQRT(r'^2-y^2) \; SQRT(r^2-y^2)) \; dy \tag{3.2.1}$$

Ki1 is the first order Bickley-Naylor function corresponding to
the general formulation

$$Kin(x) = \int_0^{\pi/2} exp(-x/cosv) \, cos^{n-1}v \, dv \qquad (3.2.2)$$

r_{least} is the least of the two radii r and r'. $\tau_1(y)$ and $\tau_2(y)$ are the optical distances shown in Fig. (II.2).

The symmetric property

$$T_b(r,r') = T_b(r',r) \qquad (3.2.3)$$

is a direct consequence of (3.2.1). However, $T_b(r,r)$ is singular and cannot be calculated by (3.2.1).

The outgoing current I_s at the cell surface S can be expressed in the following way

$$I_s = \int_0^R 2\pi r \, Q(r) \, T(S,r) \, dr \qquad (3.2.4)$$

As shown in Appendix II referring to Fig. (II.4) the transfer function $T(S,r)$ may be expressed as

$$T(S,r) = 1/(4\pi^2 R) \int_{-r}^{r} (Ki2(\tau(\rho_1)))$$

$$+ Ki2(\tau(\rho_2)))/SQRT(r^2-y^2) \, dy \qquad (3.2.5)$$

3.3. Discretization

As originally proposed in (2) the integrals in equations (3.1.1) and (3.2.4) are performed by Gaussian quadrature over the subintervals representing the different material regions, e.g., fuel, cladding and moderator. To each Gaussian interval point, k, corresponds a Gaussian radius, r_k, a weight, W_k, including the appropriate interval length as a factor, a point flux $\phi_k = \phi(r_k)$, a point source $S_k = S(r_k)$, and a cross section $\Sigma_k = \Sigma_s(r_k)$.

In this way the integral equation (3.1.1) is transformed formally into a system of linear equations

$$\phi_k = \sum_{i=1}^{N} 2\pi r_i \, W_i(\phi_i\Sigma_i + S_i) \, T(r_k,r_i) \qquad (3.3.1)$$

In the same way I_s is expressed as

$$I_s = \sum_{i=1}^{N} 2\pi r_i W_i (\phi_i \Sigma_i + S_i) \; T(S,r_i) \tag{3.3.2}$$

3.4. The neutron balance

Because of the singularity the term $W_K \cdot T_b(r_k,r_k)$ has to be found indirectly through the neutron balance equation, which takes the form

$$1 = \int_0^R 2\pi r \Sigma(r) \; T_b(r,r') \; dr + 2\pi R \; T(S,r') \tag{3.4.1}$$

The right side expresses the probability that a neutron emitted at r' either collides in the cell or escapes.

On discrete form (3.4.1) becomes

$$1 = \sum_{i=1}^{N} 2\pi r_i W_i \Sigma_i T_b(r_i,r_k) + 2\pi R \; T(S,r_k) \tag{3.4.2}$$

from which a formal value for $T(r_K,r_K)$ satisfying the neutron balance equation can be found

$$T_b(r_k,r_k) = (1 - \sum_{i \neq k} 2\pi r_i \; W_i \Sigma_i T_b(r_i,r_k) - 2\pi R \; T(S,r_k)) / (2\pi r_k W_k \Sigma_k) \tag{3.4.3}$$

3.5. The white boundary condition

As shown in several works[6],[7] the white boundary condition in most cases are preferable when a fuel pin cell is transformed into an equivalent cylinder cell. This implies that the current I_s is reflected back into the cell as if it came from an isotropic source distributed on the surface S.

Direct derivation or reciprocity considerations lead to the following expression for the first flight flux contribution at radius r from this source

$$\phi_s(r) = I_s \; T(r,S) = 8\pi R \; T(S,r) \; I_s \tag{3.5.1}$$

The fraction of neutrons from this source which passes uncollided

through the cell is

$$A = (2\pi R \ I_S - \int_0^R 2\pi r \ \Sigma(r) \ I_S \ T(r,S) \ dr)/(2\pi R \ I_S)$$

$$= 1 - 4 \int_0^R 2\pi r \ \Sigma(r) \ T(S,r) \ dr$$

$$= 1 - 4 \sum_k 2\pi r_k \ \Sigma_k \ W_k \ T(S,r_k) \tag{3.5.2}$$

Assuming a greyness of the cell surface represented by a factor G where $0 \le G \le 1$, the escape current through repeated passages and reflections generates a surface source, Q_S equal to

$$Q_S = I_S \cdot G(1 + A \cdot G + (A \cdot G)^2 + \ldots) = \frac{I_S \ G}{1 - AG} \tag{3.5.3}$$

The matrix element $T_{ik} = T(r_i, r_k)$ corresponding to the white boundary condition can now be expressed as

$$T_{ik} = T_b(r_i, r_k) + T(S, r_k) \ \frac{G}{1 - AG} \ T(r_i, S) \tag{3.5.4}$$

As a direct consequence of (3.2.3), (3.5.1) and (3.5.4) the reciprocity property

$$T_{ik} = T_{ki} \tag{3.5.5}$$

can be derived.

3.6. Integration procedure for transfer kernels and functions

By a variable transformation $x = y/r'$ and $x = y/r$, respectively, the interval of integration in (3.2.1) and (3.2.5) is transferred into $-1 \le x \le 1$. The same singularity $1/\text{SQRT}(1-x^2)$ will appear in both cases. This makes the integrals excellently suited for Gauss-Chebyshev quadrature

$$\int_{-1}^1 f(x)/\text{SQRT}(1-x^2) \ dx \approx \sum_{i=1}^n \pi/n \ f(\cos(\pi(2i-1)/(2n))) \tag{3.6.1}$$

Since the functions $f(x)$ are even in both cases, it is convenient to choose n even, $n = 2m$, which changes (3.6.1) into

$$2 \int_0^1 f(x)/SQRT(1-x^2) \, dx = \sum_{i=1}^{m} \pi/m \, f(\cos(\pi(2i-1)/(4m)))$$

$$(3.6.2)$$

For each Gaussian radius r_k as defined in (3.3) optical distances $\tau(\rho_1)$ and $\tau(\rho_2)$ corresponding to the values $y_i = r_k \cos(\pi(2i-1)/(4m))$ is found and the appropriate term $\pi/m \, f(\cos(y_i))$ added to the sum (3.6.2).

The contribution to the integrals (3.2.1) and (3.2.5) from the $\tau(\rho_2)$-term may have singularities in its first derivative at y-values that indicate passage from one material composition to another along the y-axis. This will, however, not cause great difficulties, because the $\tau(\rho_1)$-term, which is smooth, will dominate. Practical experience has shown that $m = 10$ gives satisfactory results deviating very little from values obtained with $m = 20$.

$T_b(r_i,r_k) = T_b(r_k,r_i)$ for $r_i > r_k$ and $T(S,r_k)$ are calculated by use of this integration procedure from (3.2.1) and (3.2.5) respectively. $T_b(r_k,r_k)$ is then calculated from (3.4.3) and finally $T_{ki} = T_{ik}$ from (3.5.4).

The equations (3.1.1) transformed into

$$\phi_i = \sum_{k=1}^{N} 2\pi r_k \, W_k \, T_{ik}(\phi_k \Sigma_k + S_k) \qquad i = 1,2,\ldots.N \qquad (3.6.3)$$

is solved groupwise by the usual iterative multigroup technique.

3.7. Angular flux calculation

Owing to the cylindrical symmetry the angular flux can be presented by the following expansion

$$\phi^A(\underline{r},\underline{\Omega}) = \sum_{e=0}^{\infty} \sum_{m=0}^{e} (2-\delta_{0m}) \, \phi_{em}(r) \, \Pi_e^m(\mu) \, \cos m\phi \qquad (3.7.1)$$

where $\mu = \cos\theta$ and $\underline{\Omega}$, θ and ϕ are directed as shown in Fig. (II.3). Π_e^m is defined as follows:

$$\Pi_e^m(\mu) = (-1)^m \, SQRT((e-m)!/(e+m)!) \, P_e^m(\mu) \qquad (3.7.2)$$

where $P_e^m(\mu)$ is the associated Legendre function.

In AFG the first six non-zero components

$$\phi_{00}, \phi_{11}, \phi_{20}, \phi_{22}, \phi_{31}, \phi_{33} \qquad (3.7.3)$$

are used in the expansion of ϕ^λ.

Referring to (4) the components $\phi_{em}(r)$ may be related by way of the differential equation (9.57) on page 276. Unfortunately, there is a sign error in this formula, which should be corrected by changing the sign between first and second term inside all four parantheses.

In the present case, where both scattering and the derived sources are isotropic, we have $S_0 = \Sigma_s/(4\pi)$; $S_{00} = S(r)/(4\pi)$ whereas all the remaining terms S_e and S_{em} are zero. For Σ the transport cross section has to be taken.

The following relation between the components (3.2.3) are obtained.

$e = 0; m = 0$

$$\frac{\sqrt{2}}{3} \left(\frac{d}{dr} + 1/r\right) \phi_{11} + (\Sigma_s - \Sigma) \phi_{00} + S(r) = 0 \qquad (3.7.4)$$

$e = 1; m = 1$

$$\frac{\sqrt{3}}{5} \left(\frac{d}{dr} + 2/r\right) \phi_{22} - \frac{\sqrt{2}}{10} \frac{d}{dr} \phi_{20} + \frac{\sqrt{2}}{2} \frac{d}{dr} \phi_{00} - \Sigma\phi_{11} = 0$$

$$(3.7.5)$$

$e = 2; m = 0$

$$\frac{2\sqrt{3}}{7} \left(\frac{d}{dr} + 1/r\right) \phi_{31} - \frac{\sqrt{2}}{3} \left(\frac{d}{dr} + 1/r\right) \phi_{11} - \Sigma\phi_{20} = 0 \qquad (3.7.6)$$

$e = 2; m = 2$

$$\frac{\sqrt{30}}{14} \left(\frac{d}{dr} + 3/r\right) \phi_{33} - \frac{\sqrt{2}}{14} \left(\frac{d}{dr} - 1/r\right) \phi_{31} + \frac{\sqrt{12}}{6} \left(\frac{d}{dr} - 1/r\right)\phi_{11}$$

$$- \Sigma\phi_{22} = 0 \qquad (3.7.7)$$

Since $\psi(r,\Omega)$ cannot contain $\cos m\phi$ terms for $r = 0$, components $\phi_{11}, \phi_{22}, \phi_{31}$ and ϕ_{33} must be zero for $r = 0$. $\phi_{00} = \phi(r)/4\pi$ is known from the calculation described in 3.1 to 3.6, and ϕ_{20} is found in the following way. Defining $I_z(r)$ as the number of

neutrons passing through a surface unit perpendicular to the
z-direction at r from, say upper half space, $I_z(r)$ can be ob-
tained by integration of the six relevant terms of (3.7.1) over
$\underline{\Omega}$ in the corresponding half part of phase space. Since only
terms with $m = 0$, because of the factor $\cos m\theta$, are non-zero
the following relation involving only ϕ_{00} and ϕ_{20} can be set up:

$$\phi_{20} = 4/\pi \, I_z(r) - 4\phi_{00} \qquad (3.7.8)$$

In Appendix III is given the derivation of an integration proce-
dure from which $I_z(r)$ can be calculated by help of the transfer
kernels $TZ(r,r')$ and $LZ(r)$

$$I_z(r) = \int_0^R 2\pi r' \, Q(r') \, TZ(r,r')dr' + LZ(r)Q_s \qquad (3.7.9)$$

Renaming the variable in (3.7.4 to 7) r' instead of r we obtain
by integration from $r' = 0$ to $r' = r$

(3.7.4) multiplied by r'

$$\phi_{11}(r) = \int_0^r r'((\Sigma-\Sigma_s) \, \phi_{00}(r') - S(r)/4\pi) \, dr'/(\sqrt{2}/3 \, r) \qquad (3.7.10)$$

(3.7.5) multiplied by $(r')^2$

$$\phi_{22}(r) = 1/\sqrt{6} \, \phi_{20}(r) - 5/\sqrt{6} \, \phi_{00}(r)$$
$$+ 1/r^2 \int_0^r (5\Sigma\phi_{11}(r') + \sqrt{2}(5\phi_{00}(r')-\phi_{20}(r')))/\sqrt{3} \, dr' \qquad (3.7.11)$$

(3.7.6) multiplied by r'

$$\phi_{31}(r) = 7/(3\sqrt{6}) \, \phi_{11}(r) + 1/r \int_0^r \Sigma \, 7/(2\sqrt{3}) \, \phi_{20}(r') \, r' \, dr' \qquad (3.7.12)$$

(3.7.7) multiplied by $(r')^3$

$$\phi_{33}(r) = 1/\sqrt{15}\ \phi_{31}(r) - 7\sqrt{2}/(3\sqrt{5})\phi_{11}$$

$$+ 1/r^3 \int_0^r (14/\sqrt{30}\ \Sigma\phi_{22}(r')\ (r')^3$$

$$+ (56/(3\sqrt{10})\ \phi_{11}(r') - 4/\sqrt{15}\ \phi_{31}(r')\ (r')^2)\ dr'$$

$$(3.7.13)$$

For use in the MONSU programme the values $\phi_{em}(r)$ should be cal-
culated on the Gaussian radii r_k inside the fuel pellet and on
the radius r_{fuel} of the fuel pellet. ϕ_{00} and ϕ_{20} are known on
the Gaussiar radii. The remaining components are determined from
the equations (- 7.10 to 13) in the quoted order. The integrals
are built up stepwise using the trapezian rule on the interval
between successive Gaussian radii. To start the process the value
of the two non-zero components ϕ_{00} and ϕ_{20} has to be extrapolated
to $r = 0$.

The ϕ_{em} values on the fuel surface is found by Newton inter-
polation of the values in the Gauss points inside the fuel and
the first Gauss point outside the fuel surface.

3.8. Stucture of the AFG-program

The program AFG is written in Algol for the Burrough 6700 com-
puter and is quite general in structure.

Any number N of concentric regions can be treated. The
regions are defined by the radii RO[1:N] the region I lying be-
tween RO[I] and the preceding radius RO[I-1], formally RO[0]= 0.
The number of Gaussian points in each region is determined by the in-
teger NG[1:N]. By this the Gaussian radii RG[1:N1], $N1 = \sum_{I=1}^{N} NG[I]$
are determined.

The number, GRP of energy groups is arbitrary, but the num-
ber, NTHG of thermal groups must be specified in order to obtain
the solution of the multigroup equation. NTHG will also deter-
mine the output for the Monte Carlo calculation. The number MM
of Gauss-Chebychev points (3.6) is input as well as a greyness
factor, G (3.5). In order to improve the convergence of the iter-

ative subroutine SOLUTION a relaxation factor OMEGA is used.
Both over- and under-relaxation may in certain cases save the
convergency, but normally it is sufficient to have OMEGA = 1.

Necessary multigroup cross sections for each material region
are as follows:

Fission spectrum, universal for all regions, FS[1:GRP]. Ab-
sorption cross sections, SA[1:N,1:GRP]. Transport corrected
scattering matrices, SC[1:N,1:GRP,1:GRP]. Fission cross sections,
SF[1:N,1:GRP] and ny times fission cross sections, NSF[1:N,1:GRP].

From these data the program calculates a transport cross sec-
tion in each group and region. For each group a volume averaged
diffusion constant, DAV, is also calculated. A geometrical buck-
ling, input BUCK, takes the overall leakage into account by add-
ing to the absorption cross section in each group and region the
product of DAV and BUCK.

Since the output from AFG should normally provide the necess-
ary input for the MONSU program, the following input not used in
AFG calculations is needed.

The number of regions in axial direction, NH. The axial dis-
tances RH[1:NH] measured from the underside of a (poison) pellet.
The number of Gaussian points, NGH[1:NH] in each axial interval.
The number of poisons present, e.g. two, ^{55}Gd and ^{57}Gd. The atomic
density of the poisons DPOI[1:NPOI,1:N1H,1:N1], N1H = $\sum_{I=1}$ NGH[I].   ◆
Absorption cross sections and scattering matrices of the poison
SAPOI[1:NPOI,1:NTHG] and SCPOI[1:NPOI,1:NTHG,1:NTHG].

Although the input structure of AFG is more general, the fol-
lowing restrictions are necessary when used to produce input to
the MONSU program.

Only three radial material regions representing fuel, clad-
ding and moderator are permitted, N = 3. Only two axial subdi-
visions representing poisoned and unpoisoned fuel pellets are
permitted, NH = 2.

The input scheme of AFG is given in Appendix IV.

When the AFG calculation is finished the relevant informa-
tion for the MONSU program is written on a file called MONSUDATA
in the computer system whence it can be retrieved, when this
program is run. The structure of the MONSUDATA is given in Ap-
pendix V.

4. THE MONSU PROGRAM

4.1. General formulation

The purpose of the program is to calculate by Monte Carlo technique the flux $\emptyset_B(Q_s)$ from (2.1.1) and (2.1.3) derived from the surface source Q_s defined in (2.1.2).

In MONSUDATA generated by AFG the first six non zero angular components according to (3.7.1) of $\phi^A(\underline{r},\underline{\Omega})$ are given on the Gauss radii inside the fuel and on the radius of the fuel surface.

4.2. Geometrical frame work

The fuel cell in which the M.C. calculation takes place (Fig. 4.1) is bounded by the cylindrical cell boundary and two planes of symmetry perpendicular to the cell axis. One plane divides the poison pellet in two symmetrical parts and one plane does the same to the interval between poison pellets. In the M.C. calculation all plane boundaries are treated as totally reflecting, whereas the cylindrical boundary is treated as a white boundary, compare sect. 3.5.

The fuel cell is divided in annular subregions (Fig. 4.2) in which the actual scoring takes place. These subregions are defined by dividing planes and cylinders respectively perpendicular to an concentric with the cell axis.

The distance between the dividing planes and between the dividing cylinders are scaled as the Gauss weights so that a Gaussian circle corresponding to a Gauss radius and a Gauss height is contained in each subregion.

4.3. The starters

Neutrons are started on the surface of the poison pellet. The distribution of the starters between the plane surface and the curved surface is determined by the ratio between the areas of the two surfaces. On each surface the starters are distributed over the Gaussian radii or heights respectively. The distribution is proportional to the Gaussian weights. On the curved surface these are the streight forward weights. On the plane surface these are multiplied by 2π times the corresponding Gauss radius. In this way the sum of Gauss weights corresponding to a set of
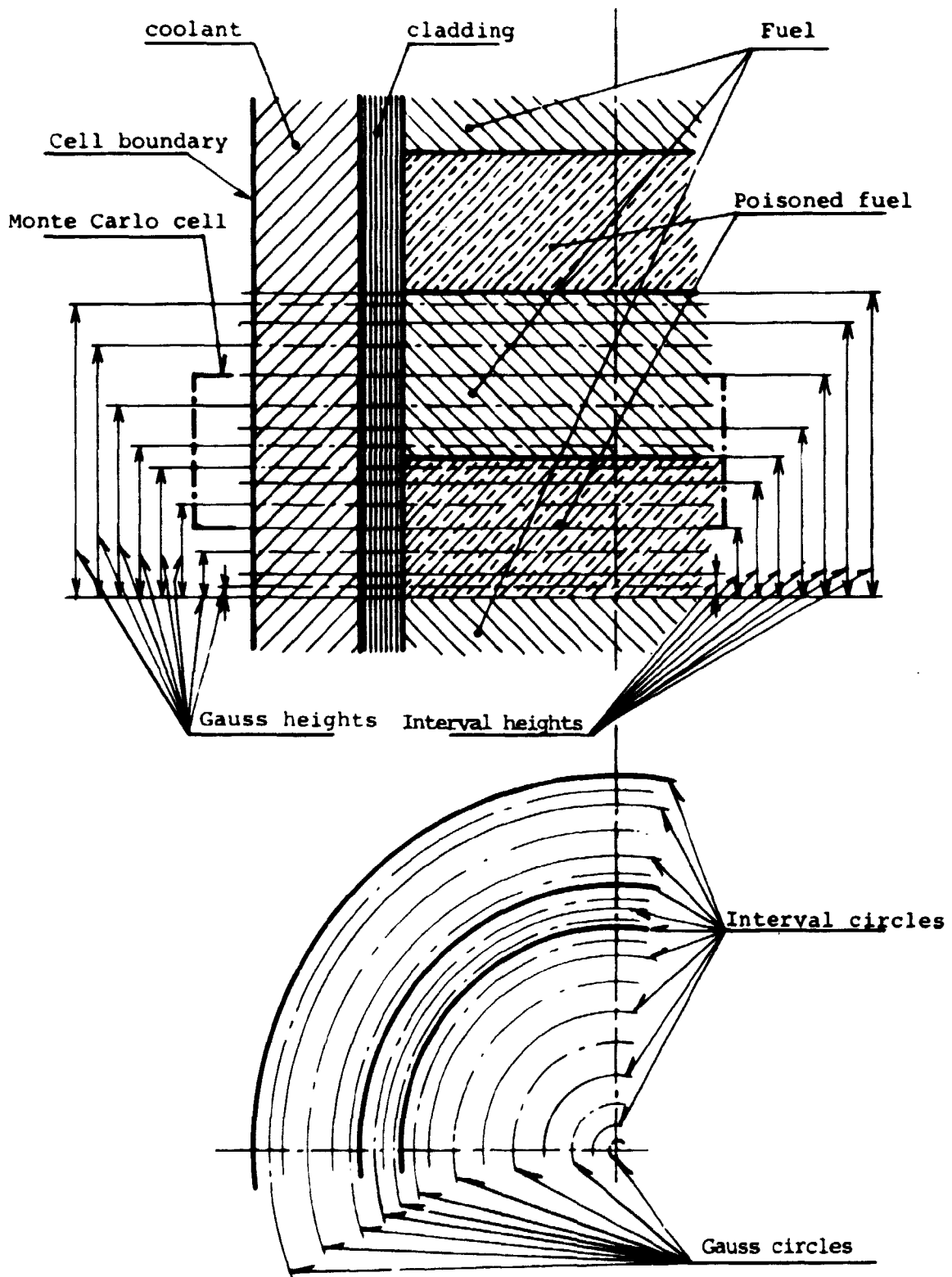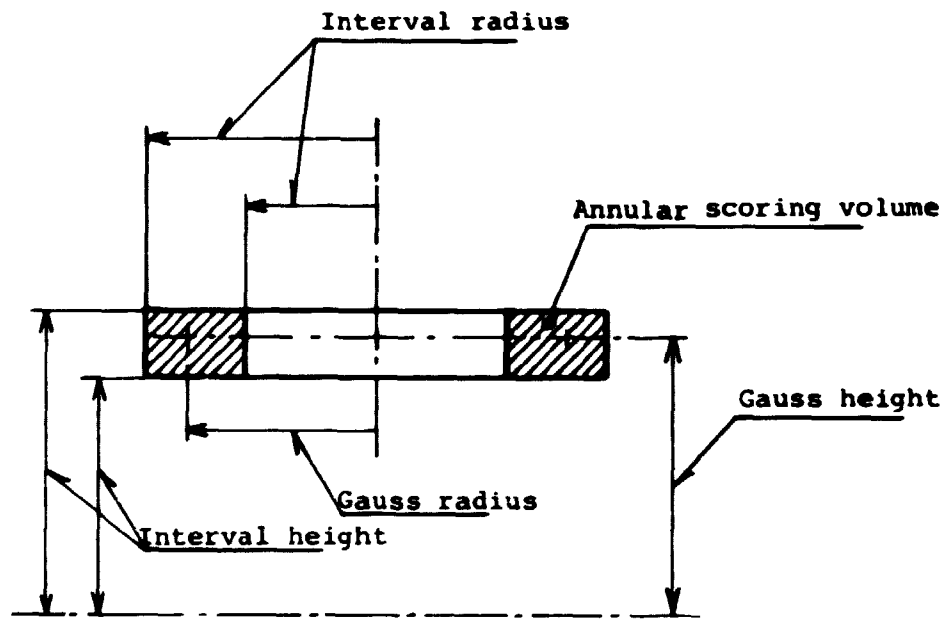
Poisoned fuel pin cell

Fig. (4.1)

Fig. (4.2)

Gauss points declared in a region will add up to respectively the axial height and the annular cross section area of the region.

When a start height or radius has been chosen by the random process, the energy group is chosen also by random process its probability being proportional to the ϕ_{00} values of the particular Gauss point. Then the direction into the poison pellet is found randomly from a cosine distribution. When the direction is determined the starter is weighted with the angular flux according to (3.7.1). For each start into the poison pellet a start is also generated in the opposite direction weighted with the appropriate angular flux and according to (2.1.2) with negative sign.

4.4. Tracing procedure

The subsequent tracing of the fate of the starters is conventional. However, since the AFG result is based on the transport cross section concept, the M.C. procedure has to be based on the same concept. Thus the track length is determined by the transport cross section, which is also used to determine the ratio between absorption and scattering. The energy group after scattering is based on the scattering matrix, which is also transport corrected, and the direction after scattering is chosen from an isotropic distribution according to the transport cross section concept.

The tracing is carried on until an absorption occurs.

4.5. The flux scoring

To get an estimate of the flux picture, the entire configuration is subdivided in annular-shaped scoring regions, and by aid of a suitable flux estimator the flux scorings in each region and for each energy group is recorded. After a final statistical processing estimates of mean fluxes and their variances is obtained.

The problem is to choose an unbiased flux estimator which has a reasonable overall efficiency. Absorption or collision estimators will be inefficient when the regions are thin. For the present work an estimator based on the track length will probably be the best choice. The socalled 'modified track length estimator' will in most cases be able to reduce the variance. It works in the following way:

A scoring track in a region begins when either the neutron enters the region from outside or emerges from a scattering collision (or a source point) inside the region. In any case, let D be the actual deposited track length and D_{max} the distance along the flight track to the prospective point of escape. Three possibilities exist:

1) $D = D_{max}$, passage: Scoring $=$ D.

2) $D < D_{max}$, scattering: Scoring $=$ D.

3) $D < D_{max}$, absorption: Scoring $= \dfrac{1-e^{-\Sigma_t D}(\Sigma_t D+1)}{\Sigma_t(1-e^{-\Sigma_t D})}$

Here Σ_t is the transport cross-section for the actual region and group.

We see that in the cases 1) and 2) we use the usual track length estimator. The estimator in case 3) is equivalent to replacing the actual D by an average over all values in the interval $[0; D_{max}]$ that could have been.

A discussion of this and other related estimators is found in (5).

4.6. Poison Burn up

After the flux scoring the total flux picture can be established according to (2.1.1) and (2.1.2). Inside the poison pellet the flux is used in each region to determine the number of poison atoms which are burned away during a specified time step. From this new poison cross sections are calculated resulting in new absorption cross sections in each poison subregion. A new M.C. round can now be started of course based on the same AFG results as before.

No fuel burn up is taken into consideration during this burn up history. However the AFG-MONSU program is only used to check and fit other more approximate procedures of simulating the axial heterogeneous poison distribution.

This approximation may consist in concentration of the poison
in a homogeneous cylinder of smaller radius than the fuel and to
fit this radius and the poison density until the best possible
agreement with the MONSU-results is obtained. For this purpose
the burn up of the fuel is not essential.

4.7. Structure of the MONSU program

The MONSU program is written in FORTRAN IV. The program is strongly
CPU time consuming. Trial calculations show that with a numerical
uncertainty of 5% by fresh GD-poisoning increasing to 10-15% un-
certainty by the end of the GD-burn away each burn up step of
2.5 days (fluxtime 0.33E + 19 - 1.20E + 19) demands 3000 sec
CPU-time on the B6700 computer. A complete burn up history will
use 50-75 steps of each 2.5 days.

This has necessitated the introduction of a RESTART/DUMP
procedure in the program. Since intermediate dump data can be
analysed by auxiliary programs it is recommended to dump after
each time step.
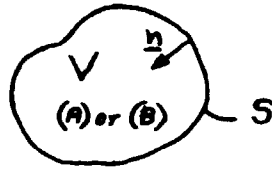
The input scheme of MONSU is given in Appendix VI.

REFERENCES

(1)   B. Fredin, private communication.

(2)   K. Kobayashi and H. Nishihara, The Solution of the Integral
      Transport Equations in Cylindrical Geometri using Gaussian
      Quadrature Formula. J. Nucl. Energy AVB 18 (1964) 513-522.

(3)   I. Carlvik, Integral Transport Theory in One-dimensional
      Geometries. AE-227 Stockholm 1966.

(4)   A.M. Weinberg and E.P. Wigner, The Physical Theory of Neu-
      tron Chain Reactors. The University of Chicago Press 1958.

(5)   J. Spanier and E.M. Gelbard, Monte Carlo Principles and Neu-
      tron Transport Problems. Addison-Wesley, Reading Mass 1969.

(6)   Y. Fukai, Zur Randbedingung mit isotroper Reflexion bei der
      Berechnung des Zylindrichen Zellenvand. Nuklonik 7 (1965)
      144-152.

(7)   Z. Weiss and R.J.J. Stammler, Calculation of disadvantage
      factor for small cells. Nucl. Sc. Eng. 19 (1964) 374-377.

APPENDIX I

Nomenclature

(C)

$$\phi^+ = \phi(\underline{r},\underline{\Omega}) \quad \text{for} \quad (\underline{\Omega}\cdot\underline{n}) > 0$$

$$\left.\begin{array}{l}\\ \\ \phi^- = \phi(\underline{r},\underline{\Omega}) \quad \text{for} \quad (\underline{\Omega}\cdot\underline{n}) < 0 \end{array}\right\} \quad r \in S$$

General equation. $M(\underline{r}) \ \phi(\underline{r},\underline{\Omega}) = q(\underline{r},\underline{\Omega})$

Definition of ϕ^A and ϕ^B

$$\text{for } \underline{r} \notin V \quad M_C \phi^A = q_C. \qquad M_C \phi^B = q_C$$

$$\text{for } \underline{r} \in V \quad M_A \phi^A = q_A \qquad M_B \phi^B = q_B$$

Assume ϕ^A and ϕ^B unique when continuous. Let ϕ_B satisfy

$$M_C \phi_B = 0 \quad \text{for} \quad \underline{r} \notin V \quad (\phi_B^+)_{ext} = (\phi_B^+)_{int} - (\phi^{A+})$$

$$M_B \phi_B = q_B \quad \text{for} \quad \underline{r} \in V \quad (\phi_B^-)_{ext} = (\phi_B^-)_{int} - (\phi^{A-})$$

The function

$$\phi_{B1} = \begin{cases} \phi^A + \phi_B & \text{for } \underline{r} \notin V \\ \phi_B & \text{for } \underline{r} \in V \end{cases}$$

have the properties

$$M_C \phi_{B1} = q_C \quad \text{for } \underline{r} \notin V$$

$$M_B \phi_{B1} = q_B \quad \text{for } \underline{r} \in V$$

ϕ_{B1} is continuous since $(\phi_{B1}^+)_{ext} = (\phi_{B1}^+)_{int}$ and $(\phi_{B1}^-)_{ext} = (\phi_{B1}^-)_{int}$.

Hence $\phi_{B1} \equiv \phi^B$ in all space   q.e.d.

APPENDIX II

The starting point is the integral transport formulation

$$\phi(\underline{r}) = \int_{v'} dv' \, Q(\underline{r}') \, \exp(-\tau(\underline{r}-\underline{r}'))/4\pi(\underline{r}-r')^2 \qquad \text{(II.1)}$$

where $Q(r')$ is the total emission density at position $\underline{r}'$, and $\tau(\underline{r}-\underline{r}')$ is the optical distance based on the transport cross section between positions $\underline{r}$ and $\underline{r}'$.

(II.1) is specialized to the cylindrical symmetric case where $\phi(\underline{r}) = \phi(r)$ is the flux at radius r produced by an emission density $Q(\underline{r}') = Q(r')$ lying outside radius r i.e. $r' > r$.

Referring to Fig. (II.1) we have

$$dv' = (\rho \cdot d\phi/\cos\alpha) \cdot dz \cdot dr'$$

$$dz = (\rho/\sin\theta) \cdot d\theta/\sin\theta$$

$$dv' = \rho^2 d\phi d\theta \cdot dr'/(\sin^2\theta \cdot \cos\alpha)$$

$$(\underline{r}-\underline{r}')^2 = \rho^2/\sin^2\theta \qquad \tau(\underline{r}-\underline{r}') = \tau(\rho)/\sin\theta = \tau(r',\phi)/\sin\theta$$

$$\phi(r) = \int_r^R Q(r') \, dr' \int_0^{2\pi} d\phi/\cos\alpha \int_0^\pi d\theta \, (\rho/\sin\theta)^2 \cdot \frac{\exp(-\tau(\rho)/\sin\theta)}{4\pi(\rho/\sin\theta)^2}$$

$$\text{(II.2)}$$

Remembering (3.2.2)

$$\phi(r) = \int_r^R Q(r') \, dr' \int_0^{2\pi} d\phi/\cos\alpha \, 1/(2\pi) \, \text{Kil}(\tau(r',\phi)) \qquad \text{(II.3)}$$

Referring to Fig. (II.2) we introduce the variable transformation

$$y = r\sin\phi \qquad dy = r\cos\phi \, d\phi \qquad d\phi = dy/\text{SQRT}(r^2-y^2) \qquad \text{(II.4)}$$

$$\cos\alpha = \text{SQRT}(1-(\sin\phi \cdot r/r')^2) = \text{SQRT}(1-(y/r')^2) \qquad \text{(II.5)}$$

$$\phi(r) = \int_r^R Q(r') \, dr' 1/(2\pi) \int_{-r}^r \frac{\text{Kil}(\tau(\rho_1)) + \text{Kil}(\tau(\rho_2))}{\text{SQRT}(1-(y/r')^2) \, \text{SQRT}(r^2-y^2)} \, dy$$

$$\text{(II.6)}$$

Comparing with (3.1.1) we get for r < r'

$$T_b(r,r') = 1/(4\pi^2) \int_{-r}^{r} \frac{Kil(\tau(\rho_1)) + Kil(\tau(\rho_2))}{SQRT((r')^2-y^2) \; SQRT(r^2-y^2)} \, dy \qquad (II.7)$$

The derivation for r > r' is quite analogue and leads to

$$T_b(r,r') = 1/(4\pi^2) \int_{-r'}^{r'} \frac{Kil(\tau(\rho_1)) + Kil(\tau(\rho_2))}{SQRT((r')^2-y^2) \; SQRT(r^2-y^2)} \, dy \qquad (II.8)$$

thus establishing the reciprocity of (3.2.1).

The current I_S passing out through the cell boundary S is calculated from the angular flux $\psi(\underline{R},\underline{\Omega})$, $\underline{R} \in S$, which can be expressed as

$$\psi(\underline{R},\underline{\Omega}) = \int_{0}^{t_n} 1/(4\pi) \; Q(\underline{R}-\underline{\Omega}t) \; \exp(-\tau(t)) \, dt \qquad (II.9)$$

where $Q(\underline{R}-\underline{\Omega}t) = Q(r)$ is the emission density, $\tau(t)$ the optical distance along the $\underline{\Omega}$ direction and $(\underline{R}-\underline{\Omega}t_n)$ the point on S lying in the $-\underline{\Omega}$ direction.

I_S can then be expressed as

$$I_S = \int d\underline{\Omega}(\underline{\Omega}\cdot\underline{n}) \int_{0}^{t_n} 1/(4\pi) \; Q(r) \; \exp(-\tau(t)) \, dt \qquad (II.10)$$

Referring to Fig. (II.3) we have

$$d\underline{\Omega} = \sin\theta \; d\theta \; d\phi$$

$$(\underline{\Omega}\cdot\underline{n}) = \sin\theta \; \cos\phi$$

$$dt = dr'/(\sin\theta \; \cos\alpha)$$

$$\tau(t) = \tau(\rho)/\sin\theta = \tau(r,\phi)/\sin\theta$$

$$I_S = \int_{0}^{R} Q(r) \, dr \int_{-Arcsin(r/R)}^{Arcsin(r/R)} d\phi \; \cos\phi/\cos\alpha \; 1/4\pi$$

$$\times \int_{0}^{\pi} (\exp(-\tau(\rho_1(\phi)) + \exp(-\tau(\rho_2(\phi))) \sin\theta \; d\theta$$

$$= \int_{0}^{R} Q(r) \, dr \; \frac{1}{2\pi} \int_{-Arcsin(r/R)}^{Arcsin(r/R)} d\phi \; \cos\phi/\cos\alpha \; (Ki2(\tau(\rho_1))+Ki2(\tau(\rho_2)))$$

$$(II.11)$$

Referring to Fig. (II.4) we introduce the variable transformation

$$y = R \sin\phi \quad dy = R \cos\phi \, d\phi \quad \cos\alpha = SQRT(1-(y/r)^2) \qquad (II.12)$$

$$I_S = \int_0^R Q(r) \, dr \; 1/(2\pi R) \int_{-r}^{r} \frac{Ki2(\tau(\rho_1)) + Ki2(\tau(\rho_2))}{SQRT(1-(y/r)^2)} \, dy \quad (II.13)$$

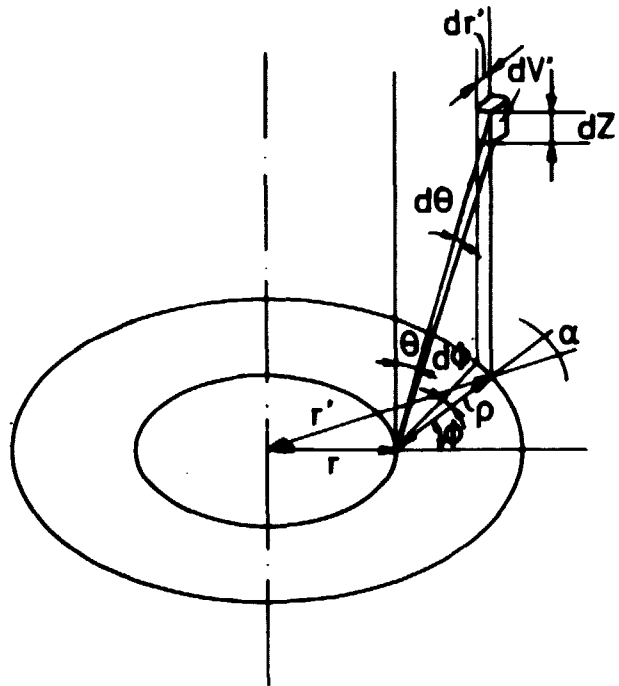Comparing with (3.2.4) we obtain the expression (3.2.5) for $T(S,r)$.
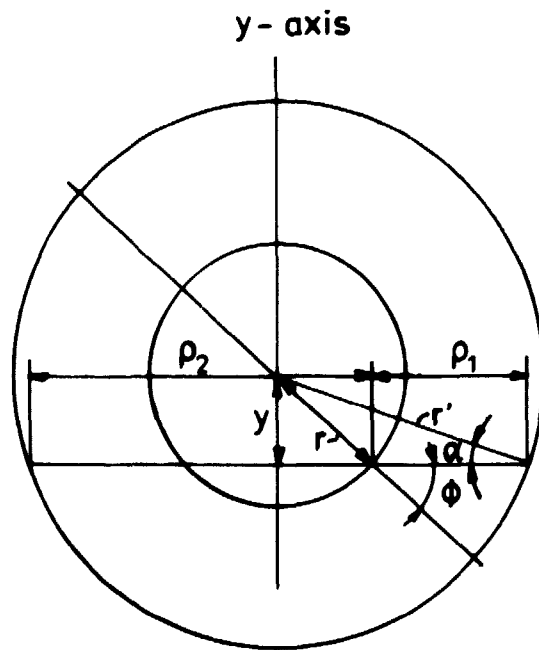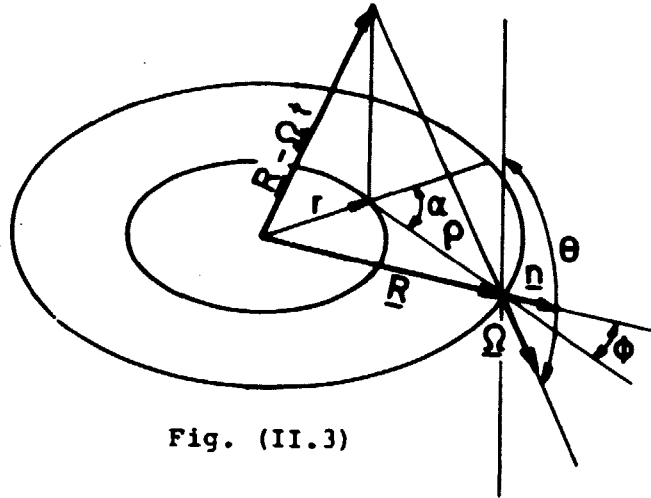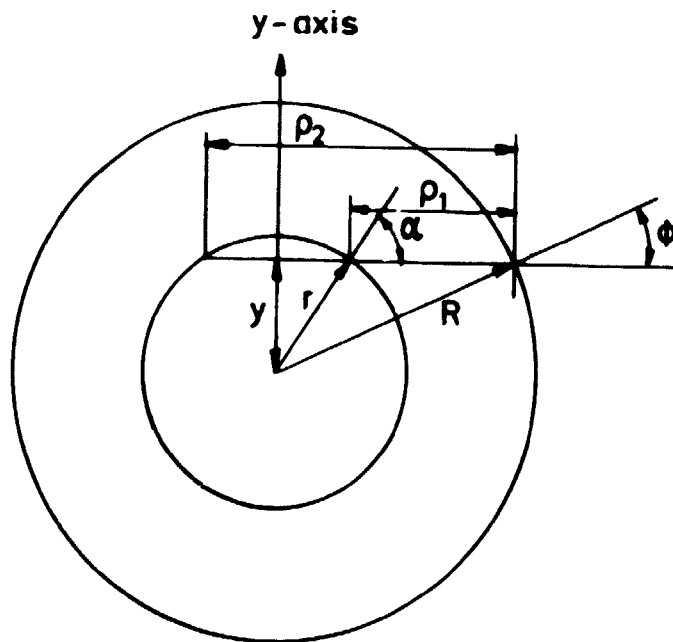
Fig. (II.1)

y - axis

Fig. (II.2)

Fig. (II.3)

Fig. (II.4)

APPENDIX III

The current I_z in (3.7.9) is calculated in the following way referring to Fig. (III.1).

The number of neutrons from source $Q(r')$ in volume element dV' which passes through surface element df at r perpendicular to the z-direction is

$$(Q(r') \ dV') (df \ \cos\theta/(\rho/\sin\theta)^2)/(4\pi) \ \exp(-\tau(\rho)/\sin\theta)$$

$$dV' = (\rho d\phi/\cos\alpha) \cdot dZ \ dr'$$

$$dZ = d\theta(\rho/\sin\theta)/\sin\theta$$

Consequently the current I_z^V derived from the volume source $Q(r')$ for $r < r'$ can be expressed as

$$I_z^V(r) = \int_r^R dr' \ Q(r') \int_{-\pi}^{\pi} d\phi/\cos\alpha \ 1/(4\pi) \int_0^{\pi/2} d\theta \ \cos\theta \ \exp(-\tau(\rho)/\sin\theta)$$

$$= \int_r^R dr' \ Q(r') \ 1/(4\pi) \int_{-\pi}^{\pi} d\phi/\cos\alpha \ E_2(\tau(r',\phi)) \qquad \text{(III.1)}$$

where $E_n(x)$ is the exponential integral defined as

$$E_n(x) = \int_1^\infty \exp(-xt)/t^n \ dt = \int_0^{\pi/2} d\theta \ \exp(-x/\sin\theta) \ \cos\theta \ \sin^{n-2}\theta$$

$$\text{(III.2)}$$

performing the same variable transformation (II.4) and (II.5) as in Appendix II, we get referring to Fig. (II.2)

$$I_z^V(r) = \int_r^R dr' \ 2\pi r' \ Q(r') \ 1/(2\pi^2) \int_{-r}^{r} \frac{E_2 \ \tau(\rho_1) + E_2(\tau(\rho_2))}{\text{SQRT}(r^2-y^2) \ \text{SQRT}(r'^2-y^2)} \ dy$$

$$\text{(III.4)}$$

For $r > r'$ the upper boundary in the last integral is changed to r'. Comparing with (3.7.9) we find

$$TZ(r,r') = 1/(2\pi^2) \int_{-r}^{r_{least}} \frac{E_2(\tau(\rho_1)) + E_2(\tau(\rho_2))}{\text{SQRT}(r^2-y^2) \ \text{SQRT}(r'-y^2)} \ dy$$

$$\text{(III.5)}$$

The number of neutrons passing through surface element df as before, coming from the surface source Q_S of neutrons reflected isotropically on the surface element df' Fig. (III.2) is

$$(Q_S \, df \, \cos\alpha \, \sin\theta) \quad (df \, \cos\theta/(\rho/\sin\theta)^2)/\pi \quad \exp(-\tau(\rho)/\sin\theta)$$

$$df' = (\rho \, d\phi/\cos\alpha) \cdot dz$$

$$dz = d\theta(\rho/\sin\theta)/\sin\theta$$

The current $I_z^S(r)$ derived from I_S becomes

$$I_z^S(r) = Q_S \int_{-\pi}^{\pi} d\phi \, 1/(\pi) \int_0^{\pi/2} d\theta \, \cos\theta \, \sin\theta \, \exp(-\tau(\rho)/\sin\theta)$$

$$= Q_S \, 1/(\pi) \int_{-\pi}^{\pi} d\phi \, E_3(\tau(\rho))$$

After the variable transformation (II.4) we get, Fig. (II.4)

$$I_z^S(r) = Q_S \, 1/\pi \int_{-r}^{r} \frac{E_3(\tau(\rho_1)) + E_3(\tau(\rho_2))}{SQRT(r^2-y^2)} \, dy \qquad \text{(III.6)}$$

Comparison with (3.7.9) gives

$$LZ(r) = 1/\pi \int_{-r}^{r} \frac{E_3(\tau(\rho_1)) + E_3(\tau(\rho_2))}{SQRT(r^2-y^2)} \, dy \qquad \text{(III.7)}$$

The integrations (III.6) and (III.7) are performed in the same way as, described in 3.6, and simultaneous with the integrals (3.2.1) and (3.2.5).

The discretization of TZ and LZ is the same as described in 3.3. Because of the singularity of $TZ(r,r')$ for $r' = r$ the term $2\pi r_k \, W_k \, TZ(r_k,r_k)$ has to be calculated in a different way.

Assuming flat flux equal to 1 in the cell, which is a solution to (3.1.1) when $\Sigma_S = \Sigma$ and $S(r) = \Sigma$ in all regions, we have $I_z(r_i) = I_S = 1/4$ and (3.7.9) can be written

$$1/4 = \Sigma \, 2\pi r_k \, \Sigma_k \, W_k \, TZ(r_i,r_k) + 1/4 \, LZ(r_i) \quad i = 1, 2 \ldots N$$

from which $2\pi r_i \, W_i \, TZ(r_i,r_i)$ can be found.

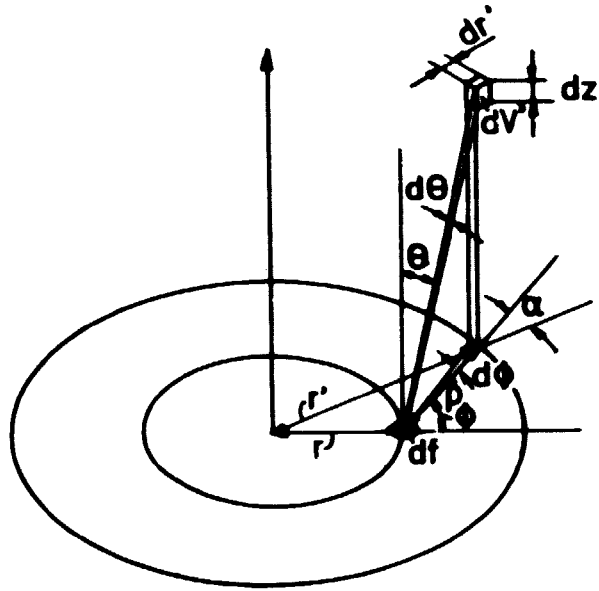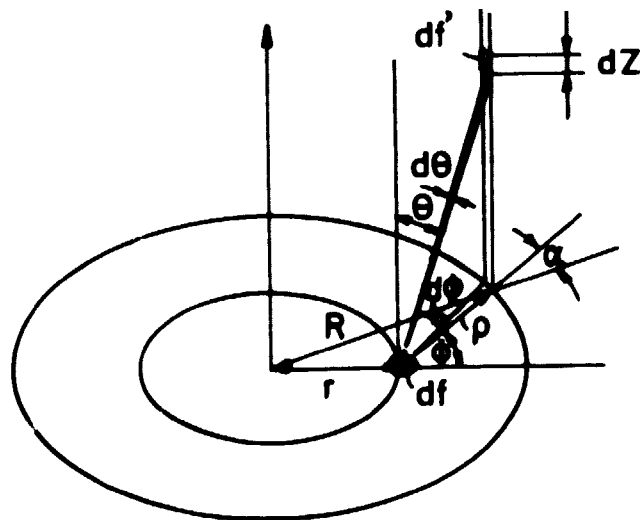Q_S is drived from (3.2.4) and (3.5.3).

Fig. (III.1)

Fig. (III.2)

APPENDIX IV

Input scheme to AFG 2

Symbol	Type	Dimension	Repetition	Specification
N	I			Number of radial regions
MM	I			Number of Gauss-Chebychev points
G	R			Greyness factor
Omega	R			Relaxation factor
NH	I			Number of axial regions
NPOI	I			Number of poisons
GRP	I			Number of energy groups
NTHG	I			Number of thermal energy groups
BUCK	R			Geometrical overall buckling
NG	I		x N	Number of Gaussian points in each radial region (not more than 7)
RO	R			Outer radius of radial region
NGH	I		x NH	Number of Gaussian points in each axial region (not more than 7)
RH	R			Upper height of axial region
XX	AR	GRP		Fission spectrum
SA	AR	GRP		Absorption cross section

SC	AR	GRP x GRP	x N	Scattering matrix
SF	AR	GRP		Fission cross section
NSF	AR	GRP		Ny x fission cross section
DPOI	AR	N1H x N1	⎤ x NPOI	Density at intersection of Gaussian cylinder radius RG and Gaussian planes, height RHG
SAPOI	AR	GRP		Absorption cross section of poison
SCPOI	AR	GRP x GRP	.	Scattering matrix for poison

I stands for integer variable, R for real variable and AR for
array. The quantities between two horizontal lines can be written
on the same card. NG and RO is written pairwise starting with
the innermost radial region and each pair on one card. The same
with NGH and RH starting with the lowest (poison containing) re-
gion.

XX is written for each region, because it is part of the
standard output on cards from the program CRS, but only XX from
the first region, which should be a fuel region, is transmitted
to the universal fission spectrum FS used in the actual calcula-
tions.

The energy groups are numbered from the highest energy, group
No. 1, to the lowest energy, group No. GRP.

The arrays XX, SA, SC, SF, NSF, SAPOI and SCPOI are written
in the 6E12.5 format on cards, which are normally output from
the CRS program. The remaining variables may be written in free
field format.

N1 is the sum of NG over N and N1H the sum of NGH over NH.
When producing input dates to MONSU the array DPOI should have
assigned zeros at intersections outside the poison pellet.

APPENDIX V

Structure of MONSUDATA

Symbol	Format	Repetition	Specification
N	I10		Number of radial region
NG	6I10	xN	Number of Gauss points in each radial region
NGH	6I10	x2	Number of Gauss prints in each axial region
RIB	6E12.5	xN1	Interval radius N1=NxNG
RIH	6E12.5	xN1H	Interval height N1H=NHxNGH*
RG	6E12.5	xN1	Gauss radius
WG	6E12.5	xN1	Radial Gauss weight
RGH	6E12.5	xN1H	Gauss height
WGH	6E12.5	xN1H	Axial Gauss weight
SA	6E12.5	xNTHG	Absorption Cross Section
SC	6E12.5	xNTHGxNTHG ^{xN}	Scattering Matrix
F100 F120 F111 F122 F131 F133	6E12.5	xN1	Angular Flux components on each Gauss radius
F100S F120S F111S F122S F131S F133S	6E12.5		Angular flux components on fuel surface (surface of reg. 1)

*In MONSUDATA NH is always equal to 2.

APPENDIX VI

INPUT SCHEME OF MONSU

1. Initiating run

FILE 1: output from AFG
FILE 3:

CARD 1 FORMAT (1x, A3)

AMODE "NEW" indicates an initiating run.

CARD 2 FORMAT (2I5)

NMAX blocsize of Monte Carlo sample

CPUMAX CPU time in first step.

CARD 3 FORMAT (2I5)

DT step length in next MC run

SEC CPU-time   "   "   "   "

If DT=0 dump on FILE 14

If DT>0 and SEC=0 the program stops

CARD 3 is repeated until DT>0 and SEC=0 on same card.

Output on FILE6 (lineprinter).

2. Restart run

FILE 13 restart file (dump from last step).
FILE 3

CARD 1 FORMAT (1x, A3)

AMODE "RES" indicates a restart run.

CARD 2 FORMAT (2I5)

DT step length in next MC-run

SEC CPU-time   "   "   "   "

If DT=0 dump on FILE 14

If DT>0 and SEC=0 the program stops

CARD 2 is repeated until DT>0 and SEC=0 on same card.

Output on FILE 6 (lineprinter).